Clinical Cutaneous Drug Delivery Assessment Using Single and Multiphoton Microscopy

16

Anthony P. Raphael and Tarl W. Prow

Contents

16.1 Introduction

Due to the relative complexity of confocal microscope instrumentation, the techniques are more suited for drug delivery ex vivo and within small animal models. In particular, single photon microscopy-based techniques such as confocal laser scanning microscopy (CLSM) have been used to characterize enhanced percutaneous drug delivery (e.g. iontophoresis (Tomoda et al. 2012), biolistic particle delivery (Xia et al. 2011), microneedles (Prow et al. 2010), etc.). CLSM has also been used in a range of in vivo and ex vivo animal models including mice (Prow et al. 2010; Fernando et al. 2010; Chen et al. 2012; Raphael et al. 2010), rats (Ito et al. 2012) and pigs (Dubey and Kalia 2010; Lopez et al. 2011). Multiphoton microscopy (MPM) is an additional technique that results in high-resolution imaging within biological tissues at greater depths than single photon systems. MPM combined with fluorescence lifetime imaging (FLIM) (multimodal imaging) results in information on the progression of disease and metabolic changes within the skin. The combination of MPM-FLIM to visualize and assess specific drug–cell/tissue interactions is a powerful technique. Further, combinatorial technologies are being developed with a range of non-invasive techniques being integrated with current single and multiphoton microscopes (e.g. optical coherence tomography (OCT), photoacoustic spectroscopy and Raman spectroscopy).

A.P. Raphael • T.W. Prow (✉)
Dermatology Research Centre, School of Medicine, The University of Queensland, Princess Alexandra Hospital, Translational Research Institute, Brisbane, QLD 4102, Australia
e-mail: t.prow@uq.edu.au

N. Dragicevic, H.I. Maibach (eds.), *Percutaneous Penetration Enhancers Drug Penetration Into/Through the Skin*, DOI 10.1007/978-3-662-53270-6_16

Although single and multiphoton microscopies have been well characterized within ex vivo and in vivo animal models, their use is yet to be established within clinical studies. The lack of clinical microscopy is due partly to ethical considerations such as the inability to apply for ethics (studies require clinician involvement) and shortage of volunteers. Even though many of the microscope systems being developed can be modified for in vivo work, it does not make them clinically suitable. Investigators are required to use independent microscope systems – one being for animal work and the other for human work. Another limitation to confocal microscopy is that the techniques often require fluorescent dyes that when conjugated to a drug change the drug's physical and chemical properties.

Even with the issues limiting the clinical analysis of percutaneous enhancers, there is much interest in the area. With advancement in microscopy and multimodal imaging techniques, it is expected that the clinical assessment of percutaneous drug delivery will become standard practice and important in determining the effectiveness of novel percutaneous drug delivery systems. This chapter focuses on single photon and multiphoton approaches that have been utilized in vivo within human skin addressing their advantages and limitations as potential techniques for the analysis of percutaneous penetration enhancers.

16.2 Cutaneous Applications of Single Photon Microscopy

The most relevant technique in relation to percutaneous penetration is the use of CLSM for in vitro, ex vivo and in vivo models. CLSM has the ability to restrict out-of-focus light, collecting only fluorescence signal from a single optical plane. Each plane is then processed computationally to construct three-dimensional images of the fluorescent signal. In particular, CLSM is extremely useful for observing spatial properties of molecules within cells and/or tissues, which is relevant to the field of pharmaceutical science and drug delivery (Agarwal et al. 2008; White and Errington 2005). However, the availability of current in vivo CLSM systems are limited with the two major instruments being the Optiscan Stratum™, Optiscan Ltd., Australia (designed for fluorescence imaging), and the Vivascope® 1500 and 3000 series from Lucid Inc., USA, designed for reflectance imaging but also with fluorescence capabilities (Fig. 16.1). What distinguishes these clinical microscopes from those used in the laboratory for ex vivo and in vitro analysis are their small size and portability (both companies have hand-held scanning systems). Although the microscope size limits the room available for complex optics (i.e. the excitation and collection ability), it is expected that the continual development of compact optics and lasers will result in greater functionality and downstream use of such CLSMs.

16.2.1 Characterization of Percutaneous Drug Delivery

Percutaneous drug delivery encompasses many approaches from the simple passive diffusion of small compounds through to the active delivery of much larger macromolecules. The need for enhanced percutaneous penetration has been well-established, with a range of chemical and physical techniques being developed. CLSM has played and is continuing to play an important role in validating these techniques – visualizing the delivery and distribution within the skin (Prow et al. 2010; Fernando et al. 2010). For example, in Fig. 16.2 we show the difference in delivery profiles between topical and microneedle enhanced delivery of sodium fluorescein within volunteers. By averaging the signal intensity per optical section we were able to 'map' the delivery profiles in a cross-sectional manner. This is a powerful technique because it clearly shows the influence of enhanced percutaneous delivery giving insight into distribution and penetration of the payload.

Lademann et al. (2003) investigated the use of a hand-held CLSM designed for dermatology applications (Optiscan Stratum™, Optiscan Ltd., Australia) (Lademann et al. 2003). The device was designed to be relatively simple and portable

Fig. 16.1 Volunteer being imaged with a hand-held in vivo reflectance confocal microscope (Vivascope 3000®, Lucid Inc., USA)

for ease-of-use within a clinical setting. The excitation source consisted of an argon ion laser with a wavelength of 488 nm specific for in vivo dyes curcumin or fluorescein. The two dyes were applied to male and female volunteers in either ethanol or sunscreen emulsion. Fluorescein application resulted in visualization of the different skin layers – stratum corneum, stratum granulosum, stratum basale and although of low resolution, the papillary dermis (Fig. 16.3). Lademann et al. hypothesized that using their CLSM system in conjunction with the fluorescein/ethanol solution, different skin layers could be distinguished between a healthy or diseased state (Lademann et al. 2003).

The curcumin/sunscreen emulsion was used to investigate potential penetration pathways and distribution of sunscreens within the skin. It was determined that the sunscreens accumulated around the edges of the corneocytes. Initially only the skin surface could be detected, however over time (20 min) three cell layers of the stratum corneum became visible. Additionally, the curcumin solution accumulated around the hair follicles and within the sweat glands. Interestingly, Lademann et al. were able to distinguish between active and passive sweat glands based on the distribution of the dye in or around the gland (Lademann et al. 2003). This study demonstrated that hand-held CLSMs have the potential for non-invasive clinical imaging.

The Optiscan Stratum™ has also been used as a validation tool assessing the penetration of microneedles within volunteers (Mukerjee et al. 2004; Bal et al. 2010a, b). Mukerjee et al. developed hollow and solid microneedles up to 200 μm in length with various diameters (Mukerjee et al. 2004). Solid microneedles were applied to the skin, near the first knuckle of the thumb followed by application of a 0.1 % sodium fluorescein solution. The application of the sodium fluorescein solution without microneedles resulted in no dye solution penetrating through the stratum corneum. CLSM assessment of microneedle application resulted in the visualization of successful microneedle penetration to a depth of 160 μm. Although no investigation was done on dye distribution and diffusion within the skin, the study showed that the application of Optiscan Stratum™ was a suitable technique for investigating the microneedle enhanced delivery of fluorescein.

In 2010, Bal et al. conducted a more in-depth microneedle study in volunteers using the delivery of fluorescein as a visual guide for characterizing the microneedle conduits and their closure over time (Bal et al. 2010a). Bal et al. also used the Optiscan Stratum™. The microneedle array consisted of 5 microneedles, 300 μm in length, 120 μm in diameter and a spacing of 2 mm. Bal et al. investigated the two techniques of fluorescein – microneedle application by either applying the dye to the skin prior to or after microneedle administration. After each application CLSM was used to characterize the microneedle conduit. Dye application post microneedle piercing resulted in

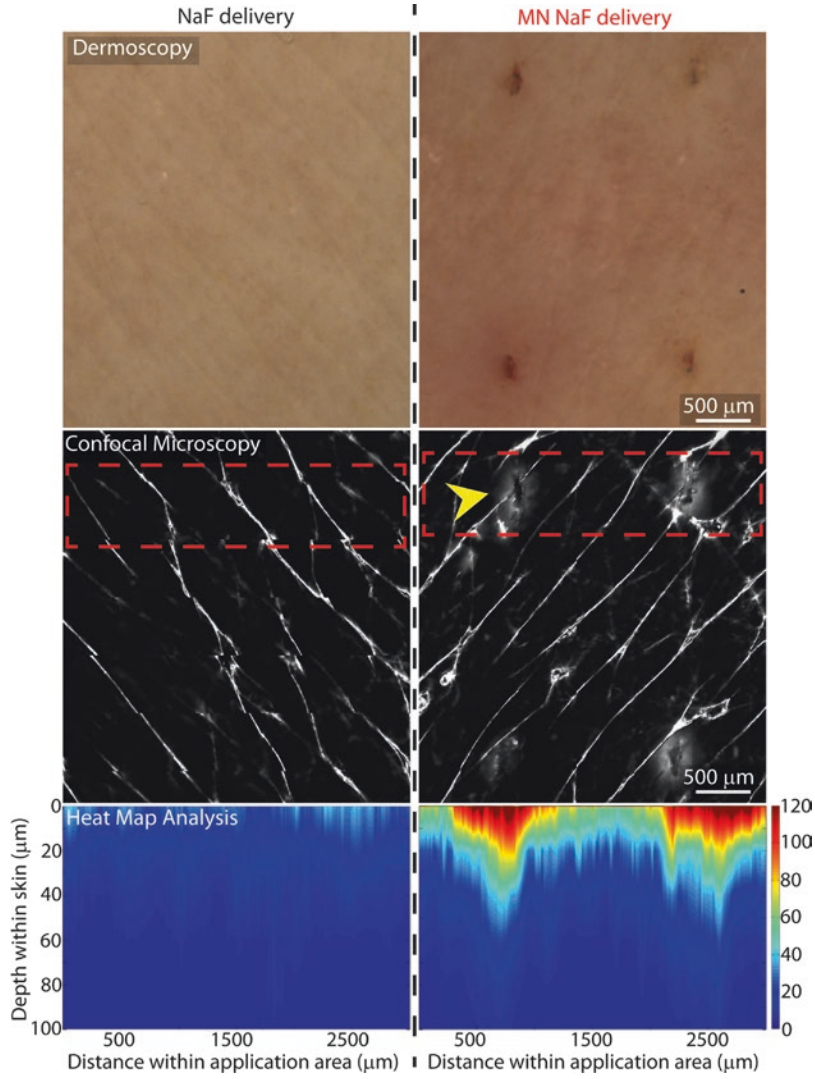

Fig. 16.2 Images showing the in vivo human delivery of sodium fluorescein (*NaF*) with and without microneedles (*MN*) using dermoscopy (*top panels*) and confocal laser scanning microscopy (*middle panels*). The bottom panels are a cross-sectional heat map representation of the average delivery profile (represented by *rectangular box*). *Arrow* indicates a microneedle deposition site

significantly higher signal than dye application prior to microneedles. Bal et al. concluded that the conduits closed within 10–15 min after microneedle application and that a depth of 150 µm was achieved (suitable for macromolecules to reach the viable epidermis (Fig. 16.4a, b)).

More recently, Vergou et al. compared the use of transepidermal water loss (TEWL) and CLSM for the in vivo characterization of the stratum corneum barrier in volunteers (Vergou et al. 2012). Once again, this study was done using the Optiscan Stratum™. TEWL is a relatively standard technique used to characterize the integrity of the epidermal barrier following disruption with percutaneous penetration enhancers. However, TEWL measurements can be influenced by internal and external factors such as humidity, temperature and air convection. Additionally, TEWL is not reliable post drug application where the drug or chemical enhancer solution is still on the skin's surface. Vergou et al. assessed the barrier integrity prior to and post treatment of dry skin (without disease) with gel and oil products (Valeo Holundergel and Valeo Dehnungspflegeoel, L'estétic GmbH, Germany) designed to rehydrate the skin following radiotherapy treatment (Vergou et al. 2012). The gel was designed to penetrate the skin – increasing hydration – followed by the oil which formed a protective layer on the skin's surface to maintain

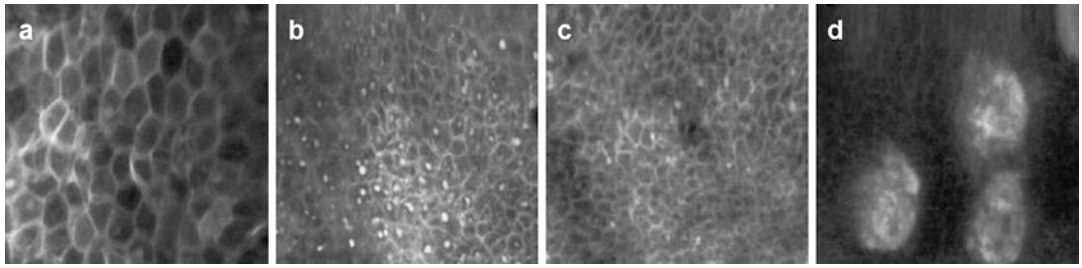

Fig. 16.3 Confocal laser scanning microscopy of sodium fluorescein within the different layers of volunteer skin: (**a**) stratum corneum, (**b**) stratum granulosum, (**c**) stratum basale, and (**d**) papillary dermis (Adapted from Lademann et al. (2003))

hydration. The products were applied twice daily on the volar forearm over a 4-week period. No treatment was done to the other arm.

Assessment was done prior, 2 weeks after and 4 weeks after application. The initial TEWL values were standardized to 100% between volunteers and it was determined that for all volunteers the TEWL for untreated skin remained constant (99±17%). The TEWL reading for the treated arm increased by 21±27% suggesting disruption of the epidermal barrier. However, stratum corneum hydration and elasticity experiments resulted in an average increase of 20% and 10%, respectively, indicating improved integrity of the epidermal barrier. CLSM showed a similar trend to the hydration and elasticity studies, where a distinct improvement in the integrity of the stratum corneum was observed. Prior to treatment the corneocytes showed an 'irregular mountainous structure'. After the 4-week treatment, the corneocytes formed a flat honey-comb pattern surrounded by intact lipid layers. Vergou et al. hypothesized that even though TEWL is non-invasive, when placed on the skin surface it disrupted the protective oil layer resulting from the treatment. Accumulated water from the gel treatment was then detected by TEWL (Vergou et al. 2012). This resulted in higher TEWL readings, which inferred a greater disruption of the stratum corneum, when in reality visual microscopic inspection showed that the stratum corneum was intact.

Overall Vergou et al. and others have shown the utility and importance of visual methods when characterizing topically applied formulations in vivo. The application and instrumentation of the described in vivo fluorescence microscopes are relatively simple to use and result in information relating to drug distribution within skin and insight into their mechanism of action. A benefit of using the Optiscan Stratum™ in relation to the investigation of percutaneous enhanced penetration is that tissue and cellular disruption can be visualized. Understanding the change in skin integrity is important for characterizing the chemical and/or physical methods used to deliver drugs. However, the limitation of the current technique is that a fluorescent solution is required to visualize the skin layers (in the previous cases, sodium fluorescein). Depending on the depth required, the fluorescent solution is injected into the skin or topically applied, potentially influencing the drug of interest.

16.2.2 Reflectance Microscopy for the Assessment of Therapeutic Changes in the Skin

Reflectance confocal microscopy (RCM) is an alternate approach to fluorescence-based CLSMs. RCM can especially be useful to characterize skin integrity and disruption as well as the change in disease state of the skin following therapeutic treatment (Ardigo et al. 2010; Segura et al. 2011; Ulrich et al. 2009). Various studies have been published characterizing the morphological changes seen in the skin over time, including studies looking at wound healing.

RCM utilizes a near-infrared diode laser as a monochromatic and coherent light source. The light source is reflected (backscattered) off the sample and passes through a pinhole aperture to

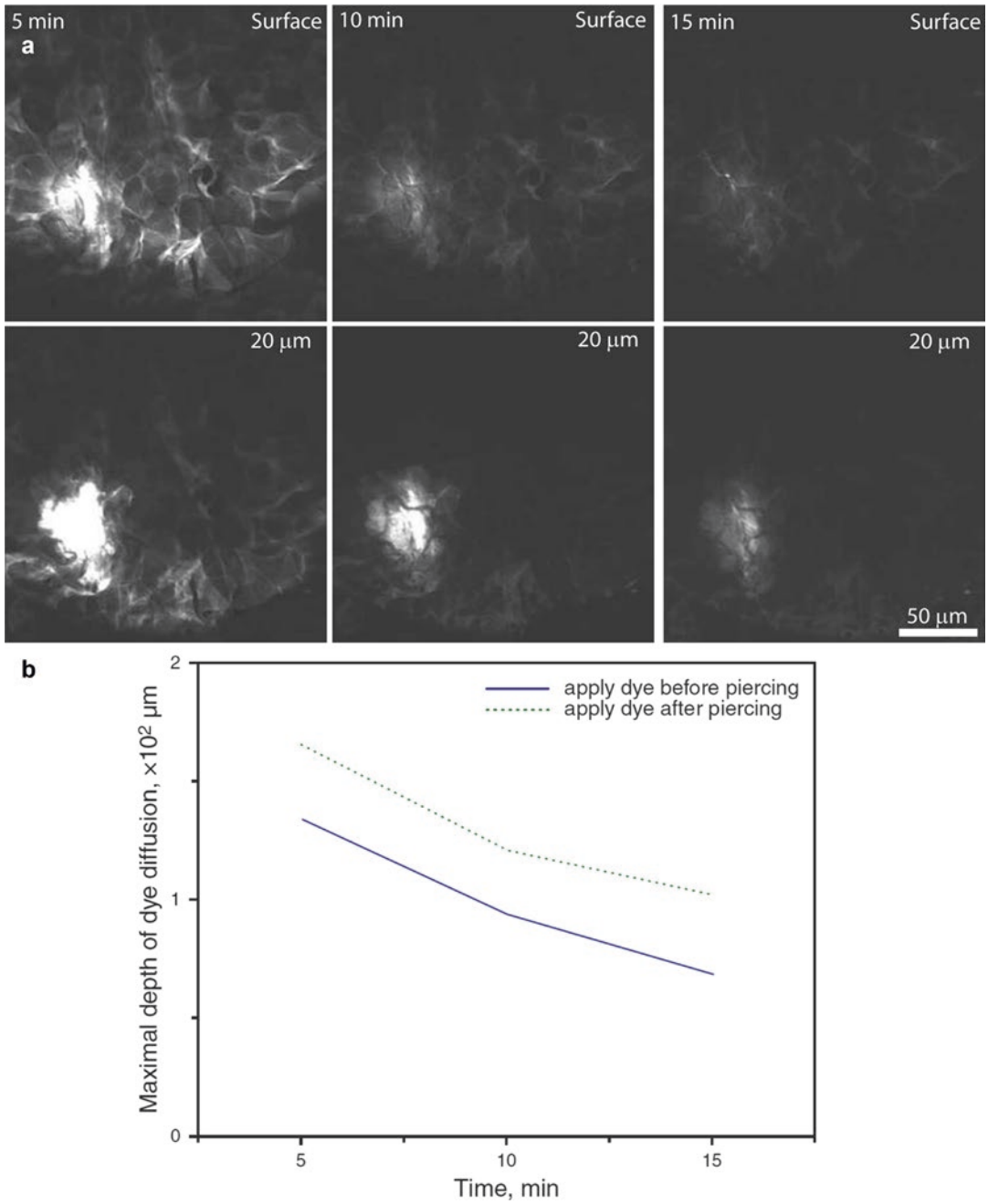

Fig. 16.4 Microneedle-enhanced delivery of sodium fluorescein in volunteers. (**a**) Confocal laser scanning microscopy of microneedle delivery 5, 10 and 15 min post application at two depths (surface and 20 µm below the surface). (**b**) Comparison maximum depth of dye diffusion over time between sodium fluorescein application before or after microneedle insertion (Adapted from Bal et al. (2010a))

the detector. RCM results in quasi-histological resolution because backscattering occurs at the edges of two biological materials with different refraction indexes – thus distinguishing cellular structures. RCM can be used for assessing structural changes within the skin in addition to serial imaging of the same site over time (Wurm et al. 2012). Furthermore, the use of near-infrared

laser sources results in relatively deep imaging down to the dermo-epidermal junction. The high cellular and structural resolution images obtained from RCM make it a valuable tool when assessing percutaneous penetration enhancers. RCM has the potential of providing information on the change in skin integrity post chemical and/or physical enhancement and unlike the previous fluorescence-based technique described it does not require a dye solution.

RCM is also used as a qualitative and quantitative technique where differences can be observed relating to the cellular and extracellular structures within skin. For example, we have investigated in the Prow group, the differences in skin from two age groups, 20–30 years and 50–60 years, respectively, using RCM (Fig. 16.5). The RCM images in Fig. 16.5b–d, f–h correspond to three distinct skin layers of interest (stratum corneum, stratum spinosum and dermo-epidermal junction). We have reported in detail and scored the RCM features associated with photo-ageing on the forearm of the two age groups (Wurm et al. 2012). We concluded that 15 statistically significant RCM features, such as furrow width/shape, keratinocyte irregularity/disarray and dermal papillae morphology could be used to quantify photo-ageing in forearm skin (Wurm et al. 2012).

One particular area that has seen much attention using RCM is the characterization and pre- and post-topical treatment of pre-cancerous and cancerous skin lesions (actinic keratosis [AK], basale cell carcinoma [BCC], squamous cell carcinoma [SCC] and melanoma). Segura et al. investigated the efficacy of photodynamic therapy (PDT) using methyl-aminolevulinate (MAL) on the treatment of BCCs (Segura et al. 2011). Six patients were treated with 1–3 cycles of MAL-PDT with each cycle consisting of two sessions of MAL-PDT 7 days apart. To enhance MAL penetration into the skin, debridement of the BCC surface was done with a curette followed by a 3 h application of MAL. The patients were assessed 1 week and 3 months post treatment using RCM with consecutive follow-ups (without RCM) every 6 months for 3 years. The RCM used was a commercially available instrument designed specifically for in vivo applications (Vivascope 1500®, Lucid Inc., USA). The system consists of a 830 nm diode laser and a 30× water immersion lens facilitating a horizontal optical resolution of 2 μm and vertical resolution of 5 μm. It was determined that RCM analysis was suitable for characterizing whether lesions underwent partial or complete remission. In these cases not all treated lesions underwent complete remission. However, those that did were characterized by the presence of normal dermal papilla and collagen fibres (Fig. 16.6).

Torres et al. published a similar study treating basale cell carcinomas (BCCs) with 5% imiquimod (Torres et al. 2004). Patients applied imiquimod 5 times daily for 2, 4 or 6 weeks, with RCM analysis at the 6-week follow-up. Torres et al. also used a Lucid Inc., USA, based RCM system designed for in vivo investigations. Whereas Segura et al. characterized the BCCs based on the skin morphology within the dermo-epidermal junction and dermis, Torres et al. focused on the keratinocyte structure and cytoplasm-to-nucleus ratio within the epidermis (Torres et al. 2004). BCCs were characterized as having elongated keratinocytes with a high cytoplasm-to-nucleus ratio compared to normal skin, which consisted of a lower ratio and regular honey-comb pattern of the cells (Fig. 16.7). Even though in this study, RCM was seen as a useful technique evaluating tumour regression in vivo without the need of surgery, there were still some limitations. The investigators felt that the technique was time-consuming (although far quicker than an invasive surgery approach). There were also technical difficulties due to movement of the relatively large scanning head, skin contact angle and maintaining contact with the skin during imaging. These limitations can be overcome with practice, however it does prevent implantation of such in vivo systems especially in laboratories that are familiar primarily with in vitro and ex vivo investigations. However, it should be noted that the RCM used was a much earlier model available from Lucid Inc. (Vivascope 1000®) and since then Lucid Inc. have developed small hand-held systems with greater ease-of-use and flexibility (Fig. 16.1).

In summary, CLSM systems are increasing in their use as non-invasive techniques for percutaneous drug delivery. Although fluorescence-based systems are limited mainly to in vitro and

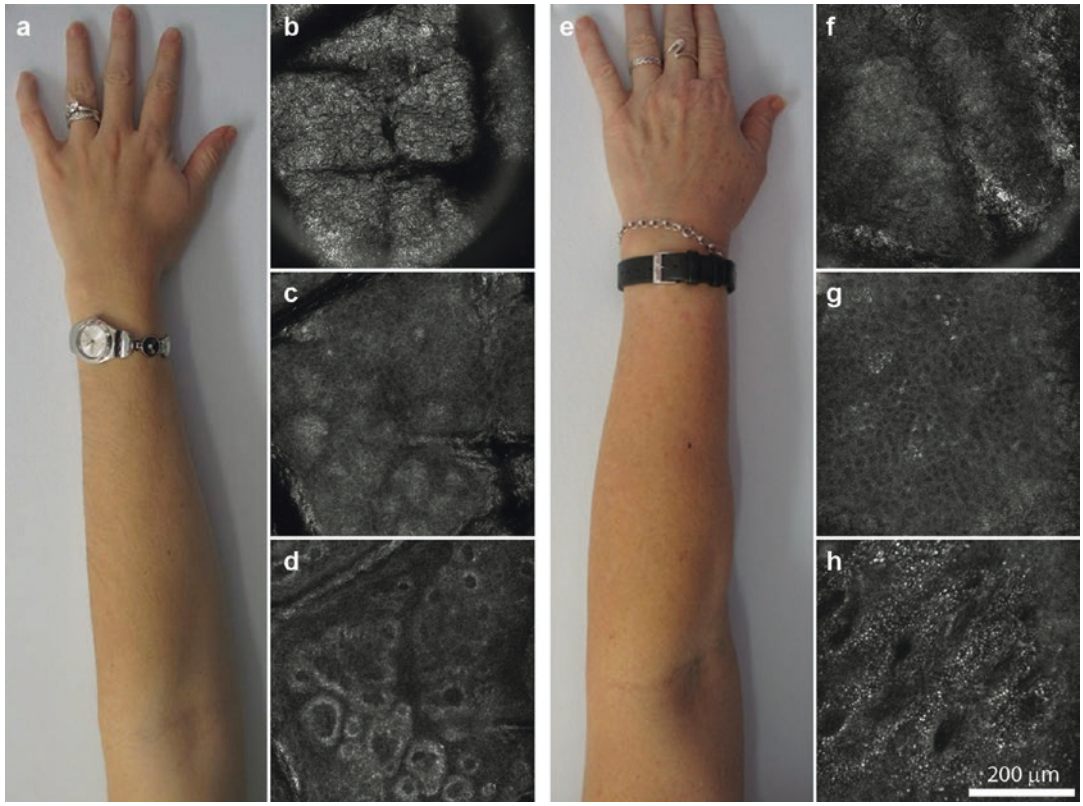

Fig. 16.5 Clinical photographs and their corresponding reflectance confocal microscopy (RCM) images. (**a**) and (**e**) show representative clinical photographs of volunteers from the two age groups, 20–30 years and 50–60 years, respectively. (**b**–**d**) and (**f**–**h**) show the corresponding RCM images of volunteers (**a**) and (**e**), respectively. (**b**) and (**f**) – stratum corneum, (**c**) and (**g**) – stratum spinosum, (**d**) and (**h**) – dermo-epidermal junction (Prow, Raphael and AR Soyer, unpublished 2012)

ex vivo applications, RCM is being utilized clinically much more due to its ability to resolve cellular and structural morphology within the skin pre and post drug application. With an increase in biocompatible fluorophores, user-friendly equipment and cost-effective instruments, it is expected that in vivo CLSM systems will continue to be incorporated into pharmaceutical and percutaneous research.

16.3 Applications of Multiphoton Microscopy

Multiphoton microscopy (MPM) is a deep tissue imaging technique that is predominantly used for non-linear two-photon excitation of fluorophores. MPM can additionally be used for three-photon excitation as well as second and third harmonic generation of biological structures. These features, combined with the fact that MPM can result in single photon sensitivity with submicron resolution has led it to being an important microscopic technique with the highest resolution in the area of non-invasive clinical imaging (Fig. 16.8) (Konig et al. 2006; JenLab GmbH).

Two-photon excitation works on the theoretical principal developed by Maria Göppert-Mayer, where two photons of similar energy interact with a molecule (fluorophore) resulting in excitation equivalent to the absorption of a single photon with twice the energy (Fig. 16.9) (Zipfel et al. 2003; Prow 2012). The probability of successful two-photon interaction (absorption) can be measured

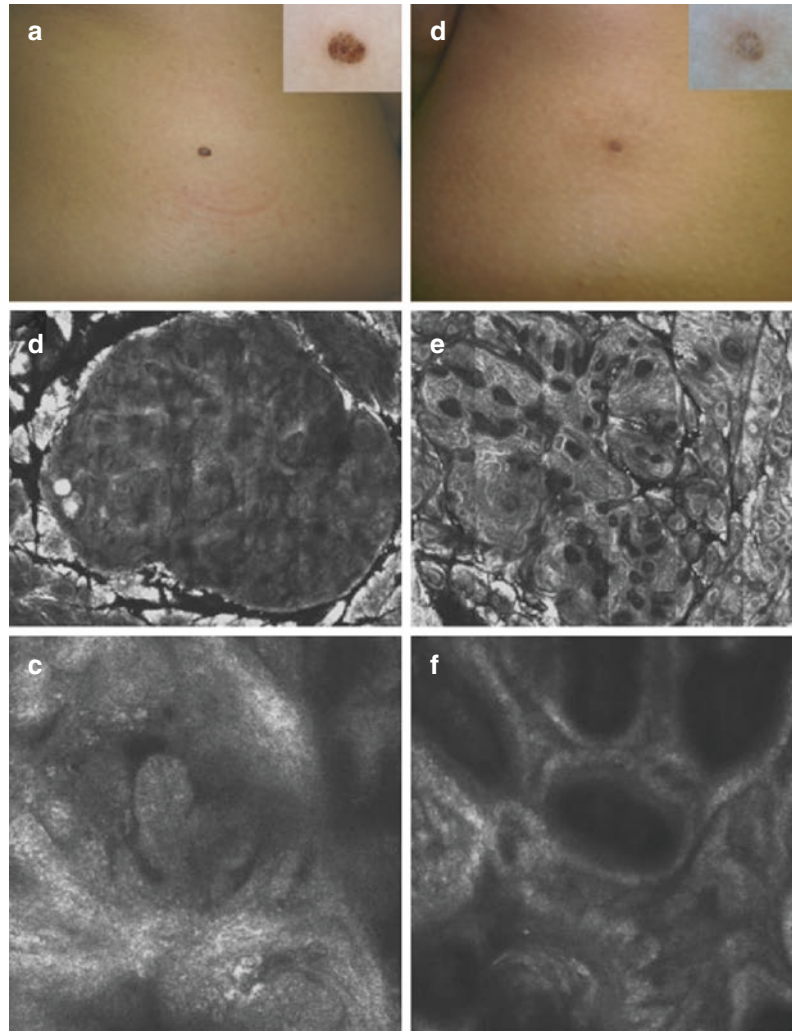

Fig. 16.6 Clinical, dermoscopy and RCM images of a 4 mm pigmented basal cell carcinoma on the abdomen of a 25-year-old woman. (**a**) Clinical and dermoscopy (*inset*) images of the lesion before photodynamic therapy. (**b**) A 4×4 mm reflectance confocal microscopy image (RCM) of the lesion prior to treatment. (**c**) Magnified image (0.5×0.5 mm) of the lesion at the dermo-epidermal junction. (**d**) Clinical and dermoscopy (*inset*) images of the lesion after two cycles of photodynamic therapy. (**e**) A 4×4 mm RCM image of the lesion after treatment showing reduction in tumour size. (**f**) Magnified image (0.5×0.5 mm) of the lesion after treatment at the dermo-epidermal junction showing the presence of normal dermal papilla (Adapted from Segura et al. (2011))

quantitatively by the two-photon cross-section (σ_{2p}). The two-photon cross-section is referred to as Göppert-Mayer (GM) where 1 GM is equivalent to 10^{-50} cm^4s. Instead of measuring σ_{2p}, which is quite complex, the product of the fluorescence quantum yield (φ_F) and absolute two-photon cross-section is calculated, which is the two-photon 'action' cross-section ($\varphi_F\ \sigma_{2p}$) (Zipfel et al. 2003). To determine the optimal wavelength for two-photon excitation, it is useful to have an understanding of the change in $\varphi_F\ \sigma_{2p}$ values with wavelength (two-photon excitation spectra). This is because a molecule's maximum single photon excitation does not always correspond to two photon excitation with similar energy (in particular symmetrical and intrinsic molecules). Therefore, when selecting fluorescent tracers for analysis of percutaneous penetration with multiphoton microscopy it is important to have an understanding of $\varphi_F\ \sigma_{2p}$.

For successful excitation to occur, the photons need to interact with the molecule almost simultaneously (approx. 10^{-16} s). Therefore, the probability of successful two-photon excitation is greatest within the beam area within the focal plane. Outside of the focal plane the probability drops significantly with negligible fluorescence emission. To further increase the probability of two-photon excitation and generate sufficient fluorescence for imaging, high laser powers are required. However, high laser powers are detrimental to biological samples. To address this problem, MPMs utilize a pulsed laser (most

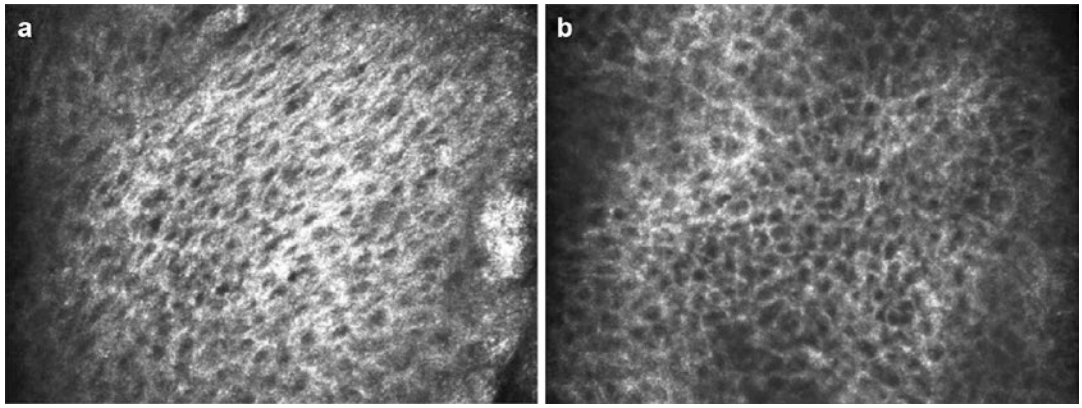

Fig. 16.7 Reflectance confocal microscopy (RCM) images of a basal cell carcinoma (BCC) before and after treatment with imiquimod. (**a**) BCC morphology prior to treatment showing elongated cells with a high cytoplasm-to-nucleus ratio (nucleus low signal, cytoplasm high signal). (**b**) BCC morphology 2 weeks after treatment showing regular honey-comb pattern and normal cytoplasm-to-nucleus ratio (Adapted from Torres et al. (2004))

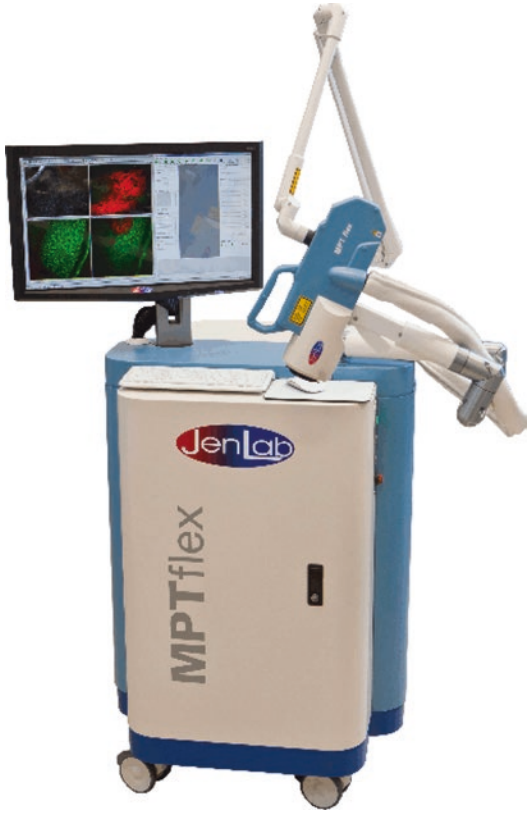

Fig. 16.8 In vivo multiphoton microscopy system (MPTflex™, JenLab GmbH, Germany) (Reprinted from JenLab website (JenLab GmbH))

commonly being a mode-locked titanium sapphire laser), which produces approx. 80 million pulses per second with a pulse duration of approx. 100 fs. The pulsed laser results in a significant increase in the probability of two photon excitation while keeping the average power relatively low. These laser power peaks contain enough dense photons to create fluorophore excitation and also retain the average power fairly low.

Seeing that molecules outside the focal plane have a low probability of successful two-photon excitation, fluorescence MPMs do not require a pinhole to reduce background noise. Absence of a collecting pinhole results in greater acquisition of emitted photons than single photon systems (Masters et al. 1997). These advantages in addition to the longer wavelengths used for MPM result in overall less scattering of the excitation beam and greater signal collection, allowing for deeper optical sectioning within specimens (approx. 2–3 times greater than what can be achieved with single photon microscopy).

16.3.1 Assessment of the Cutaneous Delivery of Nanoparticle Compounds Using Multiphoton Microscopy

Conventional imaging techniques for nanoparticle identification utilizes electron microscopy, in particular transmission electron microscopy (TEM) (Butler et al. 2012). Its high resolution (ability to

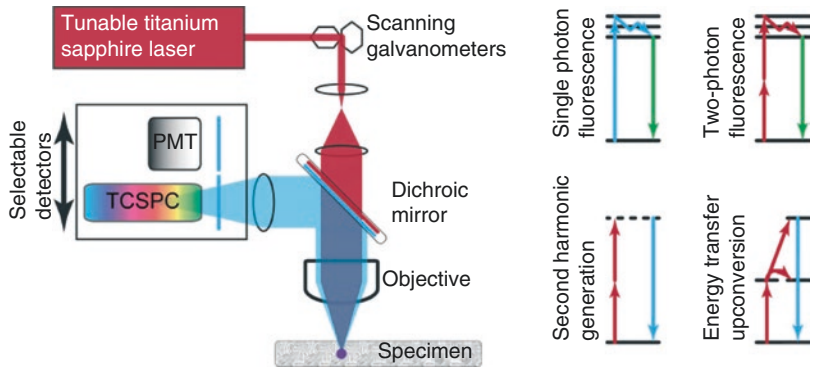

Fig. 16.9 Simplified schematic of the optical layout for multiphoton microscopy and energy transfer diagrams. Tuneable 80 MHz titanium sapphire laser sources are most commonly used for MPM. The light source is then raster scanned over the imaging area using scanning galvanometers. The dichroic mirror and objective lens then pass the excitation beam to the sample. The emission is collected and passed to one or more detectors. Photomultiplier tubes and time-correlated single-photon counting detectors can be used depending on application. Single, two-photon and second-harmonic generation Jablonksi diagrams are showed on the right (Reprinted from Prow (2012))

visualize individual nanoparticles) and ability to distinguish nanoparticles extra/intra-cellularly makes it a powerful technique in relation to nanoparticle – cell co-localization (Prow et al. 2008). However, for samples to be imaged using TEM, they must be at a thickness that allows the electrons to transmit through the sample. This is a time-consuming highly technical process that requires sectioning and embedding of the sample within resin prior to imaging. Additionally, TEM is an ex vivo microscopy technique and therefore inherent to the limitations of using an ex vivo model system to describe what is occurring in vivo.

Single photon microscopy is another technique that has been used for nanoparticle imaging both ex vivo and in vivo (Prow et al. 2006, 2008, 2012). As discussed earlier, the major advantage of this technique is its ease of use and availability of relatively inexpensive equipment. However, for the nanoparticles to be detected they need to be intrinsically fluorescent or be fluorescently labelled.

Dromard et al. conducted a study investigating the use of in vivo corneocyte imaging using a customized fibered confocal fluorescence microscope technique (Dromard et al. 2007). Briefly, an optical fibre bundle was attached to a fluorescence microscope set-up and used to image the surface of the skin. Although not assessing the delivery of nanoparticles to the skin, Dromard et al. applied fluorescein or 300 nm fluorescein embedded nanoparticles to the surface of the skin (Dromard et al. 2007). The nanoparticles accumulated preferentially around the edges of the corneocytes defining their boundaries. This approach provided a relatively simple and quick analysis of nanoparticle interaction with the surface of the skin.

MPM is one particular technique that is showing great promise as a tool for defining the risk of nanoparticle exposure (Fig. 16.10). In particular, MPM results in high-resolution deep tissue imaging within biological tissues (ex vivo or in vivo) with the ability to separate nanoparticle signals from endogenous fluorophores (although MPM is not able to resolve individual nanoparticles) (Fig. 16.10) (Prow 2012; Labouta et al. 2011; Liu et al. 2012). Furthermore, when coupled with fluorescence lifetime imaging (FLIM) and time-correlated single photon counting (TCSPC) detectors, MPM systems have the capability of distinguishing between the simultaneous excitation of nanoparticles and endogenous fluorescence within biological tissues without the need of fluorescent dyes (not possible with other techniques).

We utilized the advantages of MPM-FLIM to investigate the use of TCSPC for simultaneous monitoring of zinc oxide nanoparticles and the metabolic state of volunteer skin (without the use

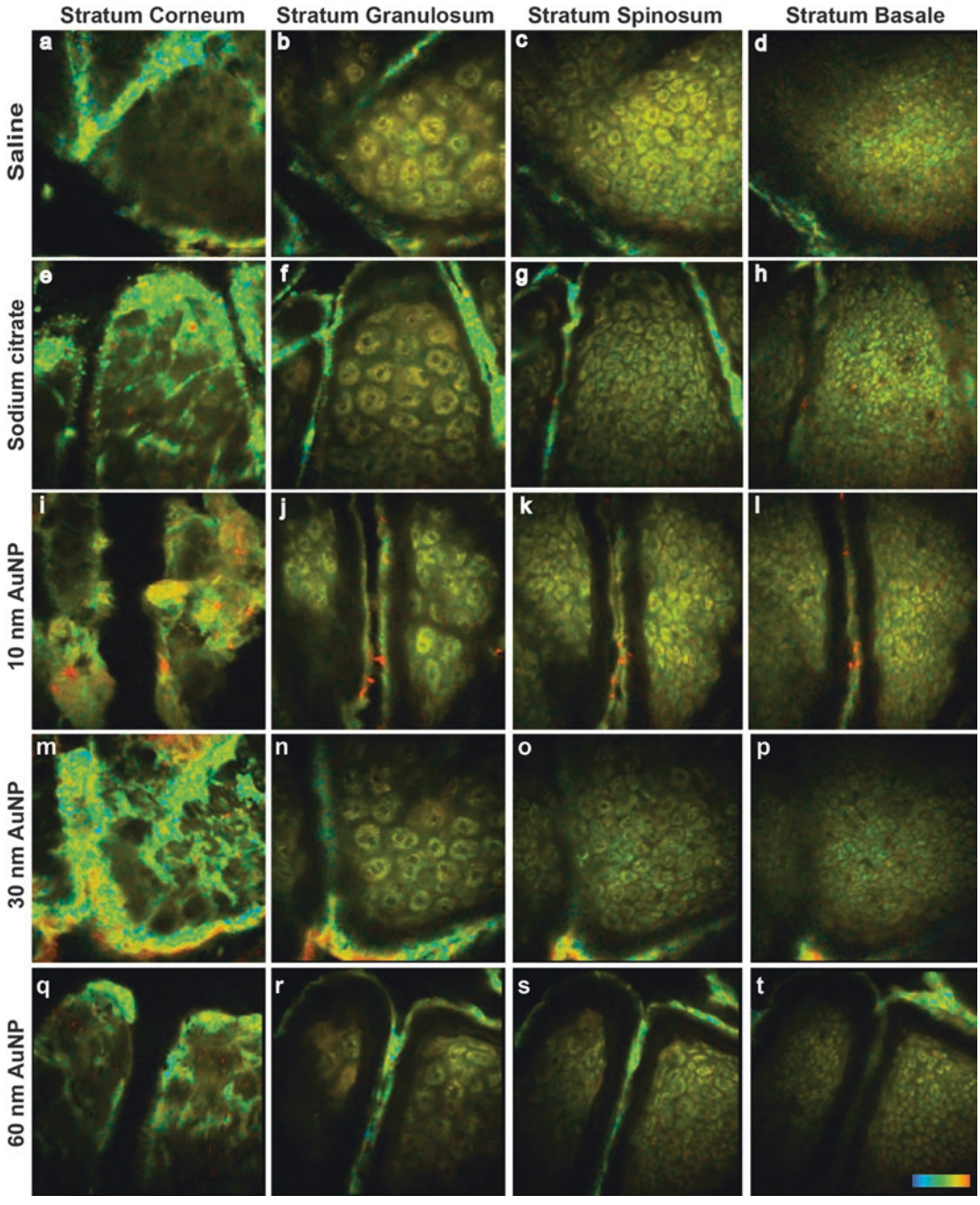

Fig. 16.10 En face multiphoton microscopy fluorescence lifetime imaging (MPM-FLIM) showing the layers of freshly excised human skin after 24 h treatment with gold nanoparticles. Nanoparticles are pseudocoloured based on signal 95–100 % (*orange to red*), skin autofluorescence is pseudoloured based on signal 0–95 % (*blue/green to yellow*) (Adapted from Liu et al. (2012)) The samples consisted of a **(a-d)** saline control, **(e-h)** sodium citrate control, **(i-l)** 10 nm gold nanoparticle treated skin, **(m-p)** 30 nm gold nanoparticle treated skin and, **(q-t)** 60 nm gold nanoparticle treated skin.

of fluorescent dyes) (Lin et al. 2011) (Fig. 16.11). The study consisted of a single healthy volunteer and eight others with psoriasis or atopic dermatitis (five with active psoriasis lesions and three with atopic dermatitis). Zinc oxide nanoparticles were applied to the forearm of healthy, tape-stripped and lesional skin. The application time for the healthy and tape-stripped skin was 4 and 24 h, but for the lesional skin only 2 h. In vivo imaging was done using a DermaInspect® MPM (JenLab GmbH, Germany) with a pulse mode-locked 80 MHz titanium sapphire MaiTai® laser. The excitation wavelength was 740 nm and the emission was filtered through a band pass filter (350–450 nm) prior to the TCSPC 830 FLIM detector. The multiphoton-excited photoluminescence (derived from the fluorescence lifetime amplitude) was used to separate the zinc oxide nanoparticle signal from the endogenous nicotinamide adenine nucleotide (NADH), also expressed as NAD(P)H signal. The microscopy set up clearly showed the zinc oxide nanoparticle distribution within the different skin types and layers (Fig. 16.11).

Roberts et al. used a similar MPM set up analysing xenobiotic transport in vivo (fluorescein and zinc oxide nanoparticles within rat liver and human skin) (Roberts et al. 2008). It was also determined that zinc oxide nanoparticles do not penetrate the skin and this was further verified using scanning electron microscopy coupled with energy-dispersive x-ray (SEM-EDX) of treated ex vivo human skin. Zvyagin et al. resulted in similar conclusions using MPM and SEM-EDX of both zinc oxide and titanium dioxide nanoparticle penetration in ex vivo and in vivo human skin (Zvyagin et al. 2008).

König et al. conducted a study using MPM to investigate the delivery and distribution of poly(lactic-co-glycolic acid) (PLGA) nanoparticles (approx. diameter of 200 nm) loaded with the antirheumatic drug flufenamic acid (Konig et al. 2006). The drug was specifically chosen because it fluoresces at 420 nm. The excitation wavelength was tuned to 720 nm to distinguish between the loaded nanoparticles compared to the unloaded controls. It was determined that like the zinc oxide and titanium dioxide nanoparticles the PLGA nanoparticles remained on the surface of the skin.

Overall MPM provides an in vivo microscopy technique that is well suited for the high resolution and deep imaging or nanoparticles within the skin. The majority of the studies using these systems within humans have focused on zinc oxide and titanium dioxide nanoparticles. This is because these nanoparticles are clinically relevant being utilized in numerous daily lotions such as sunscreens and cosmetics. It is expected that with the continual increase in nanoparticles as a percutaneous delivery enhancer, MPM will play an important role in assessing nanoparticle penetration and distribution within skin potentially providing information aiding in their clinical approval and use.

16.3.2 Analysing the Skin's Metabolic Response to Drugs Using Multiphoton Microscopy Fluorescence Lifetime Imaging

The combination of MPM with FLIM provides an in vivo microscopy technique which could potentially provide information on the progression of disease and metabolic changes within skin post drug administration (Prow 2012; Labouta et al. 2011; Liu et al. 2012; Lin et al. 2011). MPM itself is useful because it provides detailed resolution on the morphological changes of the cells (in particular keratinocytes) and also any changes to the collagen network. However, one endogenous fluorophore of particular interest is NAD(P)H (i.e. NADH and NADPH). NAD(P)H is localized within living cells, either unbound in the cytoplasm or bound to mitochondrial enzymes, and plays an important role in cellular metabolism (Sanchez et al. 2010). Depending on the cellular microenvironment (i.e. cellular metabolism), the NAD(P)H fluorescence lifetime changes, which can be detected by FLIM. Simply put, an increase in oxidation within the skin may result in an increase in unbound NAD(P)H and a decrease in bound as well as their corresponding lifetimes (unbound has a short lifetime and bound has a longer lifetime).

As discussed in the previous section, we used MPM-FLIM for simultaneous monitoring of zinc oxide nanoparticles and the metabolic state of volunteer skin (Lin et al. 2011). It was determined that

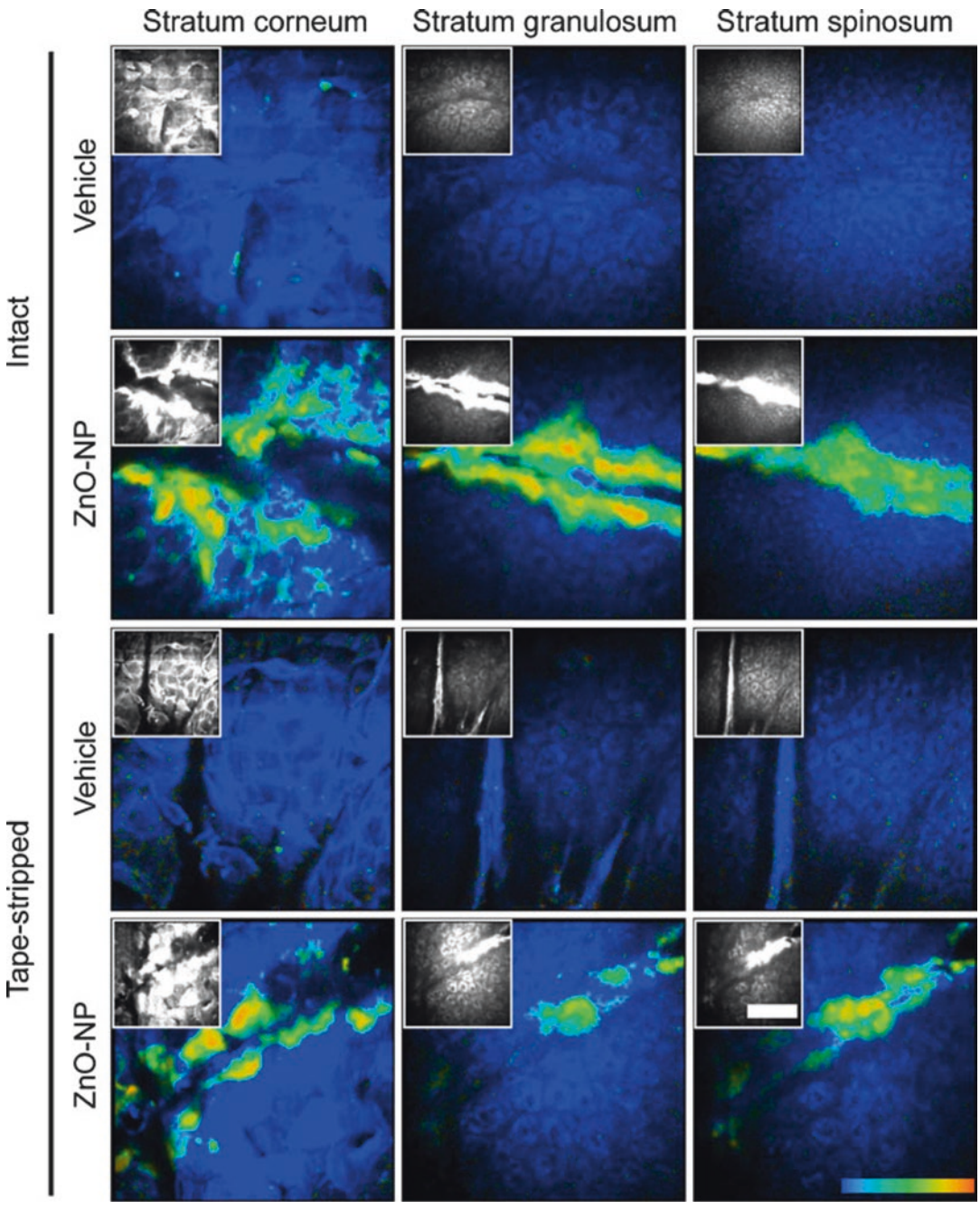

Fig. 16.11 In vivo multiphoton microscopy (MPM) images of intact and tape-stripped skin at different layers within the skin after 24 h treatment with zinc oxide nanoparticles. Nanoparticles are pseudoloured based on signal 90–100 % (*green to red*), skin autofluorescence is pseudoloured based on signal 0–85 % (*blue*). Grayscale insets show overall intensity only (Reprinted from Lin et al. (2011))

the free NAD(P)H signal increased significantly in tape-stripped skin treated for 4 h with zinc oxide nanoparticles compared to the control. However, no significant changes were detected for the lesional skin (Fig. 16.12). This corresponded to what was reported by König et al. where the application of FLIM was found to be technically challenging in thicker stratum corneum (i.e. lesional

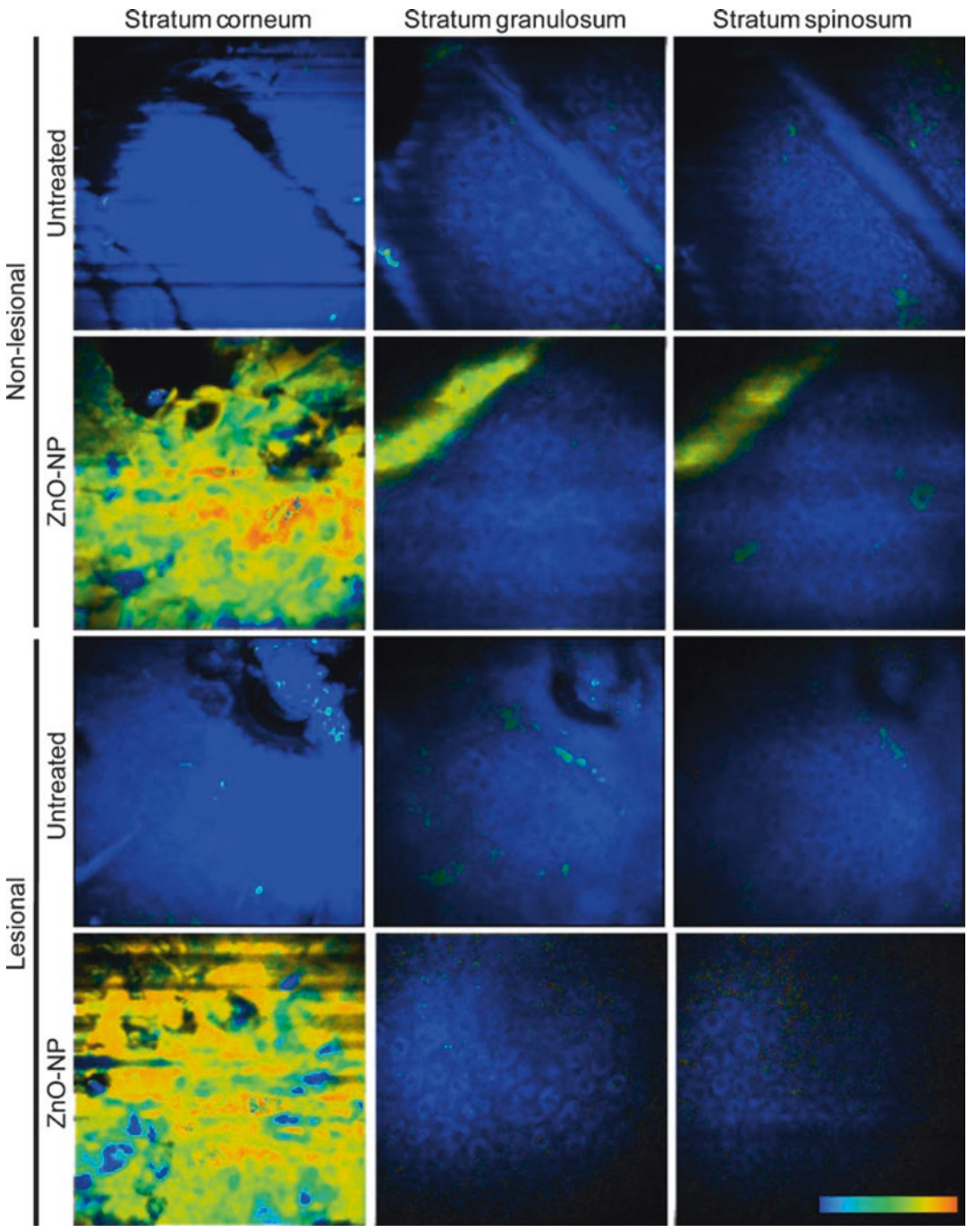

Fig. 16.12 In vivo multiphoton microscopy (MPM) images of intact and tape-stripped skin at different layers within the skin after 2 h treatment with zinc oxide nanoparticles. Nanoparticles are pseudoloured based on signal 90–100 % (*green to red*), skin autofluorescence is pseudoloured based on signal 0–85 % (*blue*) (Reprinted from Lin et al. (2011))

areas) (König et al. 2011). However, König et al. observed a greater variance in the amplitude of bound and unbound NAD(P)H lifetimes in lesional skin compared to healthy skin. The lesional coefficient of variation was largest in the stratum spinosum, being 8.1 times greater than non-lesional

areas. It is proposed that these differences in FLIM output, combined with the high resolution visual images from MPM, can be used to assess therapeutic or toxic affects following topical exposure.

16.4 Advancements in Non-invasive Analysis of Drug Delivery to the Skin Using Multimodal Imaging

Non-invasive multimodal imaging is the combination of two or more imaging techniques used within a single examination. The origins of multimodal imaging can be largely attributed to the development of combined nuclear medicine, positron emission tomography and magnetic resonance imaging. These multimodal instruments were developed due to the need for more accurate and localized imaging of drug–cell/tissue interaction in relation to neurology and oncology, in particular the longitudinal assessment of tumour progression/regression after treatment.

There is much interest in the areas of pharmaceutical science and percutaneous drug delivery for the incorporation of multimodal imaging, resulting in the development and introduction of various multimodal in vivo skin imaging techniques (Konig et al. 2009, 2010; Graf and Boppart 2012; Zhang et al. 2011). One common technique as discussed in the previous section is the use of MPM-FLIM. The significance of MPM and FLIM is that the same area of skin can be imaged with MPM and analysed by FLIM concurrently providing information-specific drug–cell/tissue interactions. However, a major challenge when combining different imaging techniques for skin analysis is that each instrument often has a different field-of-view and optical sectioning ability. Additionally, the region-of-interest within skin studies is often quite small (being limited to the size of the objective lens) making it difficult to image the exact same area of skin with different techniques.

Although not technically multimodal, König et al. investigated the use of sequential optical coherence tomography (OCT) and MPM (Konig et al. 2009). OCT is a reflectance-based technique where optically sectioned images are obtained by measuring the amplitude and the echo time delay of backscattered light. König et al. used two OCT systems (EX1301®, Michelson Diagnostics, UK and HSL-2000-10 MDL®, Santec Corp., Japan) in conjunction with the DermaInspect MPM® (JenLab GmbH, Germany) (Konig et al. 2009). To image the same area of skin between instruments, a custom metal O-ring and custom glass coverslip was developed to fit into the MPM, OCT and dermoscope (Fig. 16.13a–d). The locator was reversibly fixed to the skin using double-sided adhesive tape. The OCT provided fast low resolution wide-field cross-sectional images 5×2 mm^2 in size. This was a contrast to the high cellular resolution of the MPM images. However, MPM has a small acquisition volume approximately $0.3 \times 0.3 \times 0.2$ mm^3. It is their differences that make the two techniques complimentary, where OCT provides a wide-field image within a lesion showing potential areas of interest that can be further analysed at a much higher resolution using MPM. König et al. investigated three different skin states being hemangioma, Pemphigus vulgaris and melanocytic lesions using the combined MPM-OCT systems. It was observed that OCT was capable of identifying features of interest that when examined by MPM was shown to be significant. For example, optical biopsies of Pemphigus vulgaris resulted in regions of low signal or 'black cavities' within the skin using OCT (Fig. 16.13e). These cavities (blisters) were also observed in the MPM images showing regions absent of cells and signal (Fig. 16.13f).

The study by König et al. showed the significance of combining MPM and OCT analysis (Konig et al. 2009). However, the two systems were independent being two different instruments, limiting its utility and ease of use. Graf and Boppart addressed this issue by integrating the two systems into a single instrument (Graf and Boppart 2012). In addition, Graf and Boppart utilized optical coherence microscopy, which is a high resolution variation of OCT. The initial challenge faced when integrating the two systems was choice of laser. MPM most commonly utilizes a wave-length tuneable titanium sapphire laser with a narrow 10–20 nm optical bandwidth.

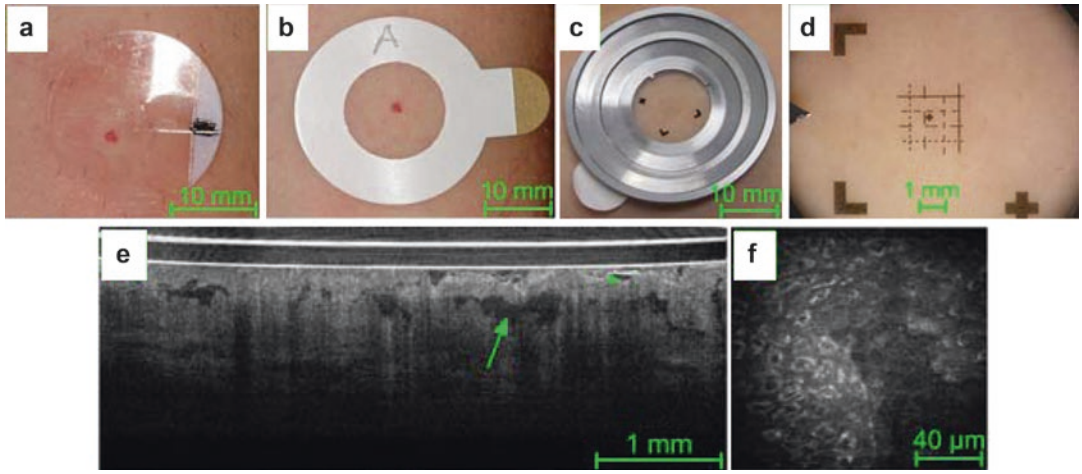

Fig. 16.13 Images of interface for alignment of dermoscope, multiphoton microscopy (MPM) and optical coherence tomography (OCT) and representative images from MPM and OCT. Interface consisting of (**a**) cover lens, (**b**) double-sided adhesive, (**c**) metal O-ring, and (**d**) coverslip with locator markings. (**e**) OCT image showing subcorneal (*) and subepidermal (*arrow*) blistering, and (**f**) corresponding MPM optical section showing subcorneal blistering (Adapted from König et al. (2009))

This is in contrast to OCM, which utilizes a broad optical bandwidth (100–200 nm) laser source. Graf and Boppart achieved excitation using a commercially available titanium sapphire dual spectrum laser source based on supercontinuum generation. The laser was integrated into the MPM-OCM system and described in detail by Graf and Boppart (2012).

The next challenge was that MPM requires a high numerical aperture (NA) lens compared to OCM which relies on the coherence length and not the NA. By separating the laser source into two beams (one for MPM and the other for OCM) Graf and Boppart were able to independently control the effective NA for both the MPM and OCM while maintaining a single objective lens (Graf and Boppart 2012). Finally the reconstruction of the collected OCM data had to be reprocessed to compensate for the coherence gate curvature so as to utilize the full field of view and integrate with the MPM images. To validate the MPM-OCM system, multiple focal areas from the dorsal hand of a human volunteer was imaged. The system resulted in high cellular resolution within the skin attributed to the MPM in addition to wide area mosaics 1×1 mm in size (Graf and Boppart 2012). The combined system provides data on both scattering and fluorescence-based contrast providing complimentary information about the state of the skin.

The combination of MPM and OCT/OCM provided a novel imaging modality assessing the cellular and extracellular structure within skin. The multimodal MPM-OCM system benefited from the high-resolution capabilities of MPM in combination with the wide-field imaging of OCM. Such MPM-based multimodal imaging techniques have potential clinical cutaneous drug delivery applications, in particular the ability to resolve cellular and structural morphology within the skin pre and post nanoparticle drug application. The continual development of multimodal systems has the potential to provide novel in vivo analytical techniques resulting in information on drug distribution and interaction within cells and tissues.

Conclusion

This chapter introduces and discusses the major imaging techniques used for the non-invasive in vivo analysis of percutaneous drug delivery. Single photon microscopy techniques to characterize percutaneous drug delivery have been well established within in vitro, ex vivo and in vivo animal models. With non-invasive clinical analysis of drug

distribution and diffusion being a major goal in the area of percutaneous drug delivery, CLSM systems are being developed to address this need, resulting in small portable fluorescence and reflectance microscopes for clinical use. Fluorescence CLSMs have the potential to provide information on drug pathways and skin barrier integrity post percutaneous enhancement. Not being restricted to fluorescence, reflectance CLSM utilizes backscattering of cellular structure within the skin to obtain structural images of tissue. RCM has been shown to be a clinically important technique – being able to resolve structural changes within skin before and after cutaneous drug delivery. The ability to assess the change in cellular morphology during treatment is an important tool, providing insight into drug/enhancer efficacy and the mechanism of action within the skin.

An alternate technique that has shown much promise in the area of non-invasive in vivo analysis is the use of multiphoton microscopy (MPM) for deep tissue imaging. A significant feature of MPM is that it can be used for second and third harmonic generation of biological structures (analysis of endogenous fluorophores within the skin). Additionally, MPM results in single photon sensitivity with submicron resolution making it one of the highest resolution techniques in the area of non-invasive clinical imaging. MPM is also unique because it has the ability to separate nanoparticle signals from the endogenous fluorophores in vivo (not possible with other systems). When combined with fluorescence lifetime imaging the technique increases its utility, being able to provide information on the progression of disease and metabolic changes within skin pre and post drug administration.

In the last decade, there has been an increase in multimodal imaging techniques (such as MPM-FLIM). The driving force behind the development of multimodal systems is to combine the advantages of individual imaging techniques potentially providing information on localization, extent and metabolic activity/functional changes within the skin following cutaneous drug delivery. For example, investigations with MPM-OCT-based systems have benefited from MPM's resolution and OCT's wide-field and imaging depth providing detailed information on structural abnormalities within diseased skin. With advances in optics and lasers it is expected that the range of diverse multimodal systems will increase providing a powerful tool set for the in vivo analysis of percutaneous drug delivery.

Overall, visualization of percutaneous delivery is a significant experimental technique providing clear information on drug distribution and optimal delivery strategies. Downstream computational image analysis extends the qualitative visualization of drug delivery to a semi-quantitative and quantitative analytical method resulting in information on drug trafficking, concentration and diffusivity within tissues – all important factors in understanding percutaneous delivery of drugs.

References

Agarwal A, Tripathi PK, Tripathi S, Jain NK (2008) Fluorescence imaging: applications in drug delivery research. Curr Drug Targets 9:895–898

Ardigo M, Cameli N, Berardesca E, Gonzalez S (2010) Characterization and evaluation of pigment distribution and response to therapy in melasma using in vivo reflectance confocal microscopy: a preliminary study. J Eur Acad Dermatol Venereol 24:1296–1303

Bal S, Kruithof AC, Liebl H, Tomerius M, Bouwstra J, Lademann J et al (2010a) In vivo visualization of microneedle conduits in human skin using laser scanning microscopy. Laser Phys Lett 7(3):242–246

Bal SM, Kruithof AC, Zwier R, Dietz E, Bouwstra JA, Lademann J et al (2010b) Influence of microneedle shape on the transport of a fluorescent dye into human skin in vivo. J Control Release 147:218–224

Butler MK, Prow TW, Guo YN, Lin LL, Webb RI, Martin DJ (2012) High-pressure freezing/freeze substitution and transmission electron microscopy for characterization of metal oxide nanoparticles within sunscreens. Nanomedicine 7(4):541–551. doi:10.2217/nnm.11.149

Chen X, Fernando GJP, Raphael AP, Yukiko SR, Fairmaid EJ, Primiero CA et al (2012) Rapid kinetics to peak serum antibodies is achieved following influenza vaccination by dry-coated densely packed microprojections to skin. J Control Release 158(1):78–84

Dromard T, Ravaine V, Ravaine S, Leveque JL, Sojic N (2007) Remote in vivo imaging of human skin corneocytes by means of an optical fiber bundle. Rev Sci Instrum 78(5):053709. doi:10.1063/1.2736346

Dubey S, Kalia YN (2010) Non-invasive iontophoretic delivery of enzymatically active ribonuclease A (13.6 kDa) across intact porcine and human skins. J Control Release 145(3):203–209

Fernando GJP, Chen X, Prow TW, Crichton ML, Fairmaid EJ, Roberts MS et al (2010) Potent immunity to low doses of influenza vaccine by probabilistic guided micro-targeted skin delivery in a mouse model. PLoS One 5(4):e10266

Graf BW, Boppart SA (2012) Multimodal in vivo skin imaging with integrated optical coherence and multiphoton microscopy. IEEE J Sel Top Quantum Electron 18(4):1280–1286

Ito Y, Hirono M, Fukushima K, Sugioka N, Takada K (2012) Two-layered dissolving microneedles formulated with intermediate-acting insulin. Int J Pharm 436(1–2):387–393

JenLab GmbH. MPTflex Multiphoton Laser Tomography. http://www.jenlab.de/MPTflex-TM.114.0.html. 31 Oct 2012

Konig K, Ehlers A, Stracke F, Riemann I (2006) In vivo drug screening in human skin using femtosecond laser multiphoton tomography. Skin Pharmacol Physiol 19(2):78–88. doi:10.1159/000091974

König K, Raphael AP, Lin LL, Grice JE, Soyer HP, Breunig HG et al (2011) Applications of multiphoton tomographs and femtosecond laser nanoprocessing microscopes in drug delivery research. Adv Drug Deliv Rev 63(4–5):388–404

Konig K, Speicher M, Buckle R, Reckfort J, McKenzie G, Welzel J et al (2009) Clinical optical coherence tomography combined with multiphoton tomography of patients with skin diseases. J Biophotonics 2(6–7):389–397. doi:10.1002/jbio.200910013

Konig K, Speicher M, Kohler MJ, Scharenberg R, Kaatz M (2010) Clinical application of multiphoton tomography in combination with high-frequency ultrasound for evaluation of skin diseases. J Biophotonics 3(12):759–773. doi:10.1002/jbio.201000074

Labouta HI, Liu DC, Lin LL, Butler MK, Grice JE, Raphael AP et al (2011) Gold nanoparticle penetration and reduced metabolism in human skin by toluene. Pharm Res 28(11):2931–2944

Lademann J, Richter H, Otberg N, Lawrenz F, Blume-Peytavi U, Sterry W (2003) Application of a dermatological laser scanning confocal microscope for investigation in skin physiology. Laser Phys 13(5):756–760

Lin LL, Grice JE, Butler M, Zvyagin AV, Becker W, Robertson TA et al (2011) Time-correlated single photon counting for simultaneous monitoring of zinc oxide nanoparticles and NAD(P)H in intact and barrier-disrupted volunteer skin. Pharm Res 28(11):2920–2930

Liu DC, Raphael AP, Sundh D, Grice JE, Soyer HP, Roberts MS et al (2012) The human stratum corneum prevents small gold nanoparticle penetration and their potential toxic metabolic consequences. J Nanomater Article ID 721706

Lopez RFV, Seto JE, Blankschtein D, Langer R (2011) Enhancing the transdermal delivery of rigid nanoparticles using the simultaneous application of ultrasound and sodium lauryl sulfate. Biomaterials 32(3):933–941

Masters BR, So PT, Gratton E (1997) Multiphoton excitation fluorescence microscopy and spectroscopy of in vivo human skin. Biophys J 72(6):2405–2412. doi:10.1016/S0006-3495(97)78886-6, S0006-3495(97)78886-6 [pii]

Mukerjee EV, Collins SD, Isseroff RR, Smith RL (2004) Microneedle array for transdermal biological fluid extraction and in situ analysis. Sensors Actuators A 114:267–275

Prow T, Grebe R, Merges C, Smith JN, McLeod DS, Leary JF et al (2006) Nanoparticle tethered antioxidant response element as a biosensor for oxygen induced toxicity in retinal endothelial cells. Mol Vis 12:616–625

Prow TW (2012) Multiphoton microscopy applications in nanodermatology. Wiley Interdiscip Rev Nanomed Nanobiotechnol 4(6):680–690. doi:10.1002/wnan.1189

Prow TW, Bhutto I, Kim SY, Grebe R, Merges C, McLeod DS et al (2008) Ocular nanoparticle toxicity and transfection of the retina and retinal pigment epithelium. Nanomedicine 4(4):340–349. doi:10.1016/j.nano.2008.06.003

Prow TW, Chen X, Prow NA, Fernando GJP, Tan CSE, Raphael AP et al (2010) Nanopatch-targeted skin vaccination against West Nile virus and Chikungunya virus in mice. Small 6(16):1776–1784

Prow TW, Monteiro-Riviere NA, Inman AO, Grice JE, Chen X, Zhao X et al (2012) Quantum dot penetration into viable human skin. Nanotoxicology 6(2):173–185. doi:10.3109/17435390.2011.569092

Raphael AP, Prow TW, Crichton ML, Chen X, Fernando GJP, Kendall MAF (2010) Targeted, needle-free vaccinations in skin using multilayered, densely-packed dissolving microprojection arrays. Small 6(16):1785–1793

Roberts MS, Roberts MJ, Robertson TA, Sanchez W, Thorling C, Zou Y et al (2008) In vitro and in vivo imaging of xenobiotic transport in human skin and in the rat liver. J Biophotonics 1(6):478–493. doi:10.1002/jbio.200810058

Sanchez WY, Prow TW, Sanchez WH, Grice JE, Roberts MS (2010) Analysis of the metabolic deterioration of ex vivo skin from ischemic necrosis through the imaging of intracellular NAD(P)H by multiphoton tomography and fluorescence lifetime imaging microscopy. J Biomed Opt 15(4):046008

Segura S, Puig S, Carrera C, Lecha M, Borges V, Malvehy J (2011) Non-invasive management of non-melanoma skin cancer in patients with cancer predisposition genodermatosis: a role for confocal microscopy and photodynamic therapy. J Eur Acad Dermatol Venereol 25:819–827

Tomoda K, Terashima H, Suzuki K, Inagi T, Terada H, Makino K (2012) Enhanced transdermal delivery

of indomethacin using combination of PLGA nanoparticles and iontophoresis in vivo. Colloids Surf B Biointerfaces 92(1):50–54

Torres A, Niemeyer A, Berkes B, Marra D, Schanbacher C, Gonzalez S et al (2004) 5% imiquimod cream and reflectance-mode confocal microscopy as adjunct modalities to Mohs micrographic surgery for treatment of basal cell carcinoma. Dermatol Surg 30 (12 Pt 1):1462–1469. doi:10.1111/j.1524-4725.2004.30504.x

Ulrich M, Krueger-Corcoran D, Roewert-Huber J, Sterry W, Stockfleth E, Astner S (2009) Reflectance confocal microscopy for noninvasive monitoring of therapy and detection of subclinical actinic keratoses. Dermatology 220:15–24

Vergou T, Schanzer S, Richter H, Pels R, Thiede G, Patzelt A et al (2012) Comparison between TEWL and laser scanning microscopy measurements for the in vivo characterization of the human epidermal barrier. J Biophotonics 5(2):152–158

White NS, Errington RJ (2005) Fluorescence techniques for drug delivery research: theory and practice. Adv Drug Deliv Rev 57:17–42

Wurm EMT, Longo C, Curchin C, Soyer HP, Prow TW, Pellacani G (2012) In vivo assessment of chronological ageing and photoageing in forearm skin using reflectance confocal microscopy. Br J Dermatol 167(2): 270–279

Xia J, Martinez A, Daniell H, Ebert SN (2011) Evaluation of biolistic gene transfer methods in vivo using non-invasive bioluminescent imaging techniques. BMC Biotechnol 11:62

Zhang EZ, Povazay B, Laufer J, Alex A, Hofer B, Pedley B et al (2011) Multimodal photoacoustic and optical coherence tomography scanner using an all optical detection scheme for 3D morphological skin imaging. Biomed Opt Express 2(8):2202–2215. doi:10.1364/BOE.2.002202

Zipfel WR, Williams RM, Webb WW (2003) Nonlinear magic: multiphoton microscopy in the biosciences. Nat Biotechnol 21(11):1369–1377. doi:10.1038/nbt899

Zvyagin AV, Zhao X, Gierden A, Sanchez W, Ross JA, Roberts MS (2008) Imaging of zinc oxide nanoparticle penetration in human skin in vitro and in vivo. J Biomed Opt 13(6):064031. doi:10.1117/1.3041492